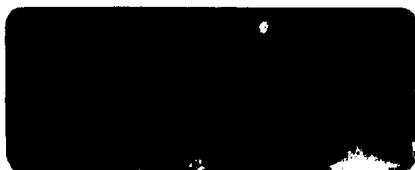


IT 93E0086 ETDE-IT--93-38
(CONF-920202--3)

ENEL

DIREZIONE STUDI E RICERCHE
CENTRO DI RICERCA ELETTRICA



Relazione
420.561/1

ETDE-IT--93-38
DE93 769322

CCMPARISON OF DIFFERENT TEST METHODS TO
ASSESS THE THERMAL STRESSES OF METAL-OXIDE
SURGE-ARRESTERS UNDER POLLUTION CONDITIONS

A.Bargigia, M.de Nigris, A.Pigini, A.Sironi

Paper presented at IEEE Winter Meeting,
New York, ²⁴~~January~~ 1992

MASTER

Gennaio 1992

DISTRIBUTION OF THIS DOCUMENT IS UNLIMITED
POWER SALES PRODUCT RB

COMPARISON OF DIFFERENT TEST METHODS TO ASSESS THE THERMAL STRESSES
OF METAL OXIDE SURGE ARRESTERS UNDER POLLUTION CONDITIONS

A. Bargigia

M. de Nigris, A. Pignini, A. Sironi
(Member) (Sr. Member)ENEL CREI
Cologno M.CESI
Milano

ITALY

INTRODUCTION

The report deals with the research conducted to assess the performance of surge arresters under pollution conditions, with special reference to the consequent thermal stress on internal active parts which can affect the energy handling capability of the arrester and may lead, in particular conditions, even to thermal runaway.

ARTIFICIAL POLLUTION TESTS

Tests were performed on multi-unit surge arresters. Several pollution methods were investigated with the aim of assessing their validity, representativity and repeatability. In particular, the following methods were applied:

- Wet contaminant with non uniform contamination
- Wet contaminant with uniform contamination
- Solid layer with non uniform contamination
- Solid layer with uniform contamination
- Salt fog test

The cumulative frequency distribution of the maximum temperature rises reached by the active parts of the arrester, ΔT , (Weibull distribution) obtained with the methods leading to significant thermal stresses is reported in Fig. 1.

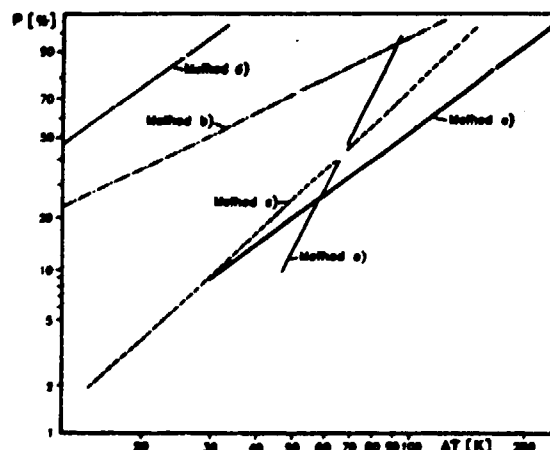


Fig. 1

The tests can be grouped into two main families:

- Those for which the voltage unbalance is forced: namely method a) and method c).
- Those for which the voltage unbalance is not predetermined and results from the pollution dynamics itself, such as method b), method d) and method e).

The first family of tests gives a lower spread in the results. Among them, method e) is less repetitive than method a) because of the spread in the humidification process. Few tests using method a) may be sufficient to assess the arrester performance. The second family of tests is characterised by a very high spread. A judgement of the surge arrester performance can be made in this case only by determining the frequency distribution of the ΔT , and this may require many tests.

ANALYSIS OF THE TEST RESULTS BY MEANS OF MODELS

The analysis of the test results was performed with the help of a physical model, set up simulating statically different possible surface conditions, and of a mathematical model implemented digitally.

The following conclusions were drawn:

- The only significant heat transfer phenomena are the radial and axial transmission within the arrester unit, while the heat transmission between the units is negligible.
- A linear relation exists when plotting the energy against the ΔT reached by the arrester in a defined time, as can be expected. A similar linear relation is also valid between the internal charge Q and ΔT at least for charge per unit time values higher than about 1 C/hour. Thus the Q value represents a good estimate of the thermal stress of the arrester; the same does not hold for the external charge Q_e .
- The local resistivity along the surge arrester unit surface is of minor importance, while the significant parameter is the overall surface resistance of the unit. The only significant current exchange between the inside and the housing of the surge arrester occurs therefore at intermediate flanges, as the current drained by stray capacitance is negligible.
- The influence of the total surface resistance of a surge arrester unit on the thermal stress was also analysed: the models confirm that the most severe contamination tests are those characterised by very different surface condition between units.

The worst situation for a two-unit arrester is when one unit is much less conductive than the other one (because of a natural dry band as in method e) or because of prefixed dry band as in method a) and c)). The charge which flows internally in the unit with the dry bands has to flow externally on the other unit and will flow up to the drying of the layer itself. The charge necessary to dry the layer is a function of the layer geometry and wetting condition and at a lower extent of the layer conductivity.

CONCLUSIONS

- The thermal performance of surge arresters under contaminated conditions mainly depends on the contamination unbalance among the arrester units and on the wetting condition while is practically not influenced by the contamination level.
- The pollution tests which force a contamination (voltage) unbalance are the most repeatable. In particular the ANSI method presents a fairly good repeatability.
- The pollution methods which do not force the voltage unbalance (those with uniform contamination and salt fog method) may be more representative of actual conditions, but are less repeatable, thus requiring a large number of tests on each object.
- The arrester heating is related to the energy (charge) which flows in the arrester blocks. The external charge has very loose relation with the arrester thermal stress, unless when it coincides with the internal charge; this happens only in the methods with a fixed contamination unbalance.

COMPARISON OF DIFFERENT TEST METHODS TO ASSESS THE THERMAL STRESSES OF METAL OXIDE SURGE ARRESTERS UNDER POLLUTION CONDITIONS

A. Bargigia

ENEL CREI
Cologno M.

M. de Nigris, A. Pignini, A. Sironi
(Member) (Sr. Member)

CESI
Milano

ITALY

Abstract Laboratory tests were carried out to investigate the thermal performance of surge arresters, under contamination and wetting environmental conditions, which lead to non uniform voltage stresses along the arresters.

The validity and repeatability of various laboratory test procedures have been examined.

The results were also analyzed by means of a mathematical and of a physical model.

Keywords Electrical Model; Pollution; Surge Arresters; Testing; Thermal Model; Thermal Stresses.

INTRODUCTION

The study of the performance of metal oxide surge arresters under pollution conditions must take into consideration three different aspects [1]...[5]:

- The strength of the external insulation.
- The effect of internal ionization that can cause premature ageing of the resistor blocks.
- The thermal stress on internal active parts due to voltage unbalance along the surge arrester axis which can affect the energy handling capability of the arrester and may lead, under particular conditions, to thermal runaway.

In spite of the fact that gapless arresters have been used for a relatively long time, a valid testing procedure to verify the above aspects has not yet been agreed upon. This reinforces the importance of further investigation and, for this purpose, intense research has been undertaken by ENEL at CESI laboratories since early 1984 to investigate all three aspects, in parallel with other similar activities around the world [3], [4], [5].

This report addresses only the research dealing with the third aspect, i.e. the thermal stresses on surge arresters under pollution. Results obtained with different artificial pollution methods were recently reported in [4] and [5], giving useful indications about the severity of the test procedures analyzed. The following points are however to be clarified:

- The order of merit of the different test methods, with special reference to their repeatability. This point is expressly addressed in the first section of this paper, which reports the results of an extensive laboratory test programme conducted with different test procedures.
- The relation between the parameters characterizing the surface conditions, the measured electrical and thermal quantities and the test severity. This point is extensively addressed in the second section of this paper, which analyses the electrical and thermal performance of a surge arrester with the support of physical and mathematical models.

SECTION 1: ARTIFICIAL POLLUTION TESTS

TEST OBJECTS AND MEASUREMENTS PERFORMED

The research was carried out considering surge arresters for maximum system voltages ranging from 145 to 420 kV.

The text only refers to the 245 kV surge arresters, which have been more systematically investigated.

The arrester was equipped with a voltage control ring and was mounted on a 1 m high pedestal. It was composed of two units connected in series through a metallic flange. Each unit was housed in a porcelain envelope with alternate sheds, having an equivalent diameter of 198 mm, and a creepage distance of 3390 mm. One column of non-linear resistor blocks, separated from the housing by an air layer of a few centimetres, was included in each unit (36 blocks in the top unit and 30 in the bottom one).

The following measurements were performed during the tests, as described in Fig. 1:

- Internal and external currents were measured by means of suitable shunts at the line terminal of the top unit and at the earth terminal of the bottom unit ($I_{l,t}$, $I_{e,t}$ and $I_{e,b}$, $I_{l,b}$, respectively). Silicon grease was used to isolate the external and internal currents. The current values were digitalized with a sampling rate of 5000 samples per second. The maximum peak values I_l , I_e (in A) recorded inside every period

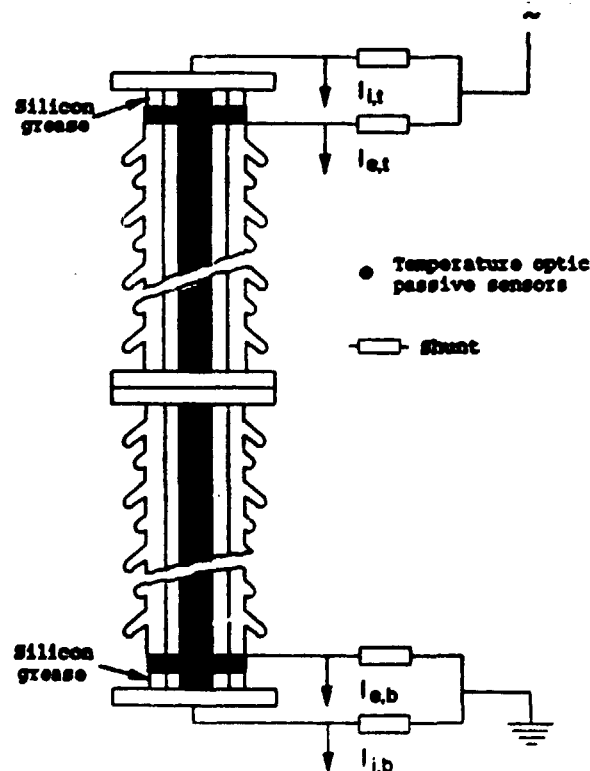


Fig. 1 Scheme of the test object, with indications of the measurements performed.

of two seconds were stored. The most significant currents and voltage waveshapes were also recorded.

- Temperatures on the blocks were measured, throughout the tests, in 7 different locations along the surge arrester using optic passive sensors. The maximum temperature rise ΔT (in Kelvin degrees: K) along the arrester was then derived.
- All the electric signals were transmitted, by means of optic fibres, to a digital data acquisition system to be stored, processed and displayed.
- Real-time acquisition software was developed to compute the electric charges on the base of the relevant currents measured: the charges Q_i and Q_e (in C) associated to the resistive component of the measured internal and external current (I_{ir} and I_{er}) were evaluated as:

$$Q_i = \int_0^t |I_{ir}| dt$$

$$Q_e = \int_0^t |I_{er}| dt$$

where t is the integration time.

The associated energies (in J) were also evaluated, when possible.

- Measurements of the volt-ampere characteristic of the arrester were made after each test series to check the integrity of the test sample.

TEST RESULTS

Different pollution methods were investigated. Test methods expressly developed for surge arresters [6], [7] were applied. Furthermore, the methods standardized for insulators [8], namely the salt fog and solid layer tests, were applied with some modifications, taking into account the peculiarities of surge arresters.

All the tests were carried out energizing the surge arrester at the voltage $U_m/\sqrt{3}$ (140 kV for the sample considered). For each method a comprehensive series of tests was carried out to analyze the influence of the most important parameters such as contamination level and test duration. Test repeatability was also systematically analyzed.

The average values and the standard deviation of the main quantities recorded during the various tests were considered.

The results were also analyzed considering a Weibull distribution of two parameters as representative of their cumulative frequency distribution. The best fitting curve and its 90 % confidence limits were determined with the likelihood methods [9].

Method a): Wet contaminant with non uniform contamination

The tests were carried out according to the procedure recommended in [6]. The arrester was first energized for one hour. Then two subsequent contamination cycles were applied, which consisted of the following phases: contamination of the bottom unit of the de-energized arrester with a slurry having a resistivity of 500 $\Omega \cdot \text{cm}$ and re-energization for a time of 15 min. The maximum voltage-off time for contamination was 10 min and the voltage was applied within 3 min of contaminant application. The arrester remained energized for another 30 min to check thermal stability. The contamination level is given in terms of slurry resistivity, as foreseen by the reference Standard [6]; to allow the comparison with other methods investigated, the Salt Deposit Density (S_{AD}) after the first contamination is given: its value was of about 0.015 mg/cm^2 ; higher values were generally found after the second contamination.

Examples of the internal and external currents ($I_{i,t}$ and $I_{e,b}$), internal and external charge ($Q_{i,t}$ and $Q_{e,b}$) and temperature rise (ΔT) as a function of time are shown in Fig. 2. The current varied from tens of milliamperes at the beginning of the first contamination cycle to a few milliamperes after 15 min. Higher values were reached in the second cycle. Correspondingly, the equivalent layer resistance passed from a few megaohm to tens of megaohm.

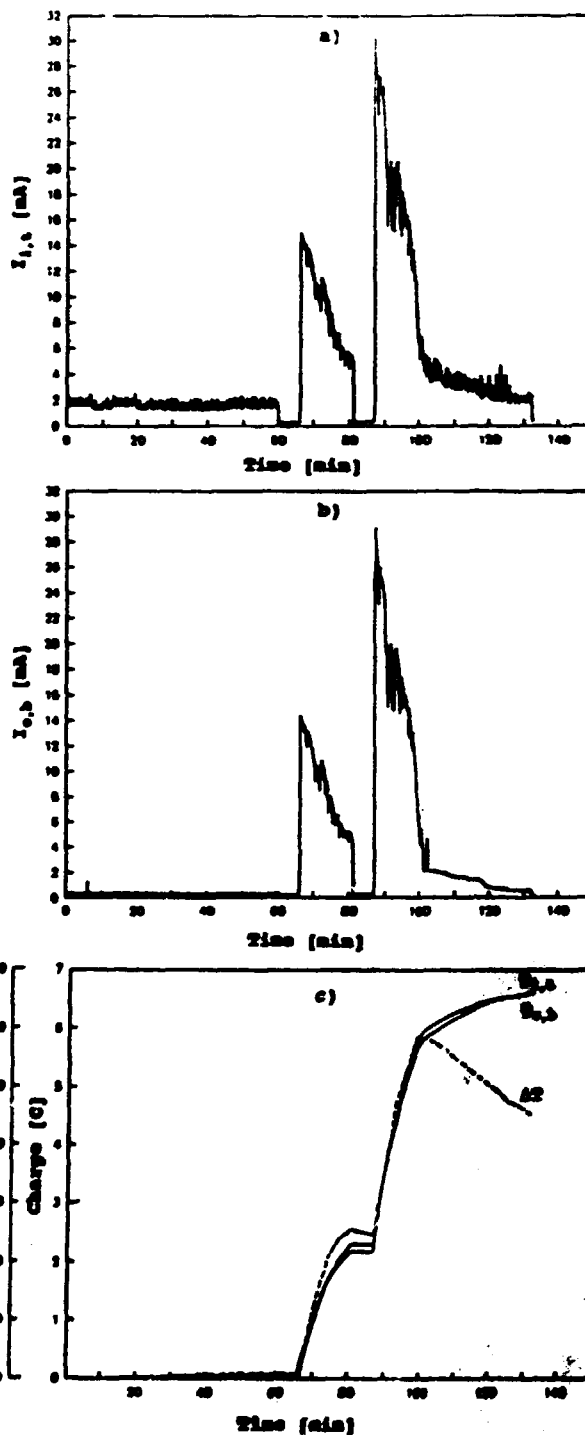


Fig. 2 Method a): examples of the trend of electrical and thermal quantities as a function of time.

The external charge on the bottom unit, $Q_{e,b}$ and the internal charge on the top unit $Q_{i,t}$ (i.e. the most stressed one) were practically equal. The charge increased mainly at the beginning of energisation. This is in agreement with the current trend, the amplitude and repetition rate of which decreases while the test continues. Sporadic high current peaks occurring when the contamination layer was nearly dry, reaching values close to the initial ones, gave a negligible contribution to the charge. The ΔT trend of the top unit closely followed that of the charge during the heating phases, with a

coefficient of proportionality of about 10 K/C. No heating was observed in the bottom unit.

The average value of the final $Q_{1,t}$ obtained in various tests was about 7 C with a standard deviation of the measured values of 1.5 C. The relatively low value of the standard deviation can be explained noticing that the charge flowing externally on the contaminated unit and internally on the other one is the charge necessary to vaporize the water contained into the contamination layer. The vaporization charge can be considered a fairly repetitive test parameter because the quantity of water is related to the physical, chemical and geometrical characteristics of the porcelain envelope with a given contamination procedure. The current trends observed in various tests also show this fact, as the area envelope of the current peaks remains nearly constant (i.e. when the pollution activity at the beginning is high, its duration is short and vice versa).

Considering the maximum value of ΔT obtained in various tests, its average value was about 70 K with a standard deviation of the measured values of 16 K.

The cumulative frequency distribution of the final values of $Q_{1,t}$ obtained in various tests is given in Fig. 3. A similar trend was found for the maximum value of ΔT .

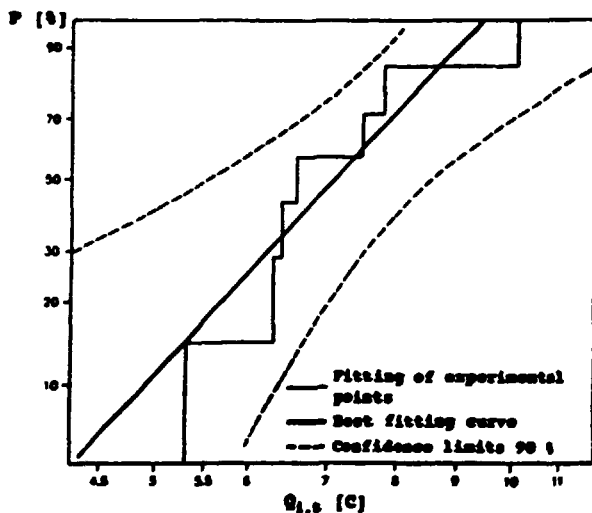


Fig. 3 Method a: cumulative frequency distribution of $Q_{1,t}$ values measured at the end of the tests.

Several tests were also performed contaminating only the top unit; the evolution of the thermal and electrical phenomena on the most stressed unit (bottom unit in the examined case) was similar to that described above except for the observed temperature rise which was a little lower than in the previous case.

Method b): Wet contaminant with uniform contamination

The procedure suggested in [7] was adopted (also reported as "slurry method" in [4]). The arrester was first energized for one hour. Then 6 subsequent contamination cycles were applied which consisted of the following phases: the arrester de-energized was contaminated uniformly with a slurry having a resistivity of 500 $\Omega \cdot \text{cm}$. The maximum voltage-off time for contamination was 10 min and the voltage was applied for 10 min after 3 min of contaminant application. Finally, the arrester remained energized for another 30 minutes to check thermal stability. The number of cycles was chosen to reach a fixed value of the maximum external charge on the bottom unit $Q_{0,b}$ of about 22 C, as suggested in [7] for a heavy / very-heavy pollution level and for the total test duration considered. The slurry resistivity was the same

as that specified for the test method a) to allow some comparison. The contamination level is given in terms of slurry resistivity; to allow the comparison with other methods investigated, the S_{40} at the end of the first contamination is given: its value was of about 0.015 mg/cm^2 ; as stated for method a), generally higher values were found after subsequent contaminations.

Examples of charge and temperature rise trends measured in the two arrester units are shown in Fig. 4 a).

Details of the $Q_{1,t}$, $Q_{1,b}$, $Q_{0,t}$ and $Q_{0,b}$ trends referring to the 4th contamination are shown in Fig. 4 b). The process can be subdivided into two phases within each contamination cycle: an initial drying phase and a subsequent thermally active phase.

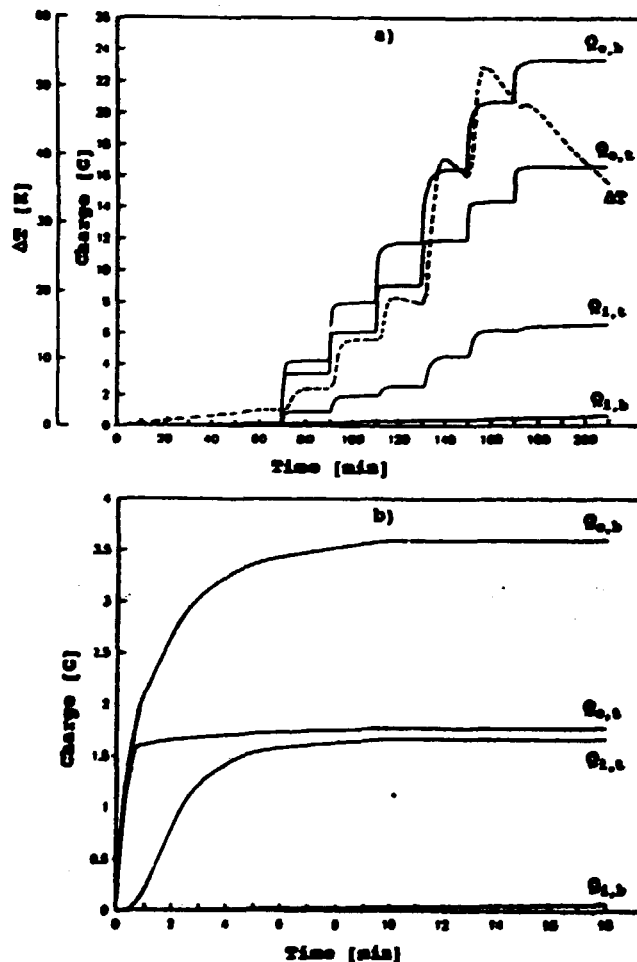


Fig. 4 Method b: example of the trend of electrical and thermal quantities as a function of time.

- a) Quantities in the whole test
- b) Quantities in the 4th cycle.

In the first phase of each cycle the current (charge) flowed mainly externally. This external current was higher than for method a) since a higher specific stress resulted on the contamination layer. This current flow dried the contamination layer. Generally, the drying effect was prevalent on the top unit. During the second phase, the current was forced to flow internally to the dried unit (generally the top one).

In the second phase of each cycle the arrester behaved as in the case of non-uniform contamination. The subsequent current however was lower than in method a) because of the drying effect caused by the initial current flow.

The ΔT of the top unit evolved during each cycle as

the $Q_{i,t}$ did, with a coefficient close to that for method a). However, because of the longer test duration, the ratio between ΔT and the $Q_{i,t}$ was lower at the end of the 6 cycles, resulting in an overall value of about 7 K/C. Also for this method, the temperature of the less stressed unit was practically unaffected by the test.

The cumulative frequency distribution of the final value of $Q_{i,t}$ and $Q_{o,b}$ reached during various tests are given in Fig. 5.

In principle, the $Q_{o,b}$ should be constant and equal to the prefixed value of 22 C. As a matter of fact, it was not possible to keep it constant, since the contamination cycles were applied in a small integer number. Its average value was 22.7 C and the standard deviation of the measured values was 2.8 C.

The internal charge $Q_{i,t}$ on the most stressed unit had a very large dispersion (average value of 5.8 C, standard deviation of 5.5 C). Fig. 5 indicates that the cumulative frequency distributions of $Q_{i,t}$ and $Q_{o,b}$ tend to converge at high probability (for $Q_{i,t}$ values having a very low probability to be exceeded). In this last condition the entire charge is injected inside the most stressed unit and the result is similar to that which would be obtained by contaminating only one unit.

The average and the standard deviation of the maximum values of ΔT were 38 K and 36 K respectively. The cumulative frequency distribution of ΔT showed a similar trend as $Q_{i,t}$. No correlation was evident between ΔT and $Q_{o,b}$, $I_{i,t}$, $I_{o,b}$, $I_{o,t}$ or $I_{o,b}$. In particular, the poor correlation between ΔT and $Q_{o,b}$ appears very clearly from the data reported: while $Q_{o,b}$ remained close to 22.8 C, ΔT varied from 14 K to 140 K.

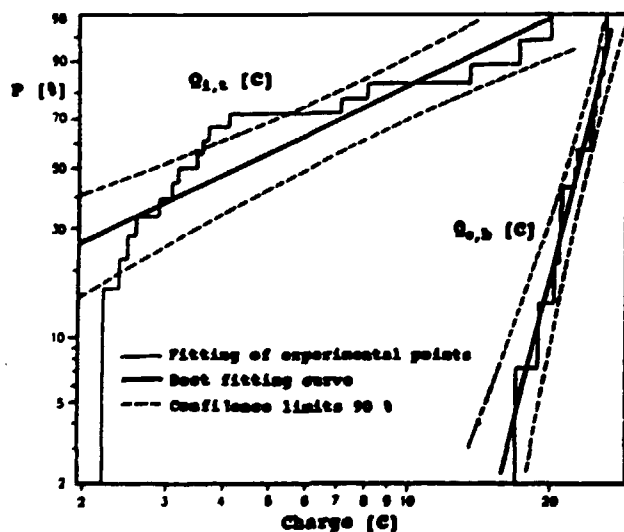


Fig. 5 Method b: cumulative frequency distribution of $Q_{i,t}$ and $Q_{o,b}$ values measured at the end of the tests.

Subsequent tests made with different contamination levels (varying the resistivity of the slurry from 50 to 500 $\Omega \cdot \text{cm}$) did not indicate any significant influence of the pollution level, at least in the examined range. This can be explained considering that the quantity of water to be vaporized was similar in all cases, even with different layer resistivities. Again, the ΔT seems more related to the method itself and to the humidification process than to the pollution level.

Method c): Solid layer with non-uniform contamination

The tests were carried out according to the test procedure B recommended in (8). In particular the test object was contaminated with the required slurry (in these tests only one arrester unit was contaminated). The object, when dry, was energized and wetted by steam fog.

The test duration was extended up to 4 hours. Salt Deposit Density, S_{sd} , values from 0.015 to 0.15 mg/cm^2 were considered.

Examples of $I_{i,t}$, $Q_{i,t}$ and ΔT measured during a test with the bottom unit contaminated are shown in Fig. 6, which refers to a value of $S_{sd} = 0.15 \text{ mg}/\text{cm}^2$ and to a test duration of 2 hours.

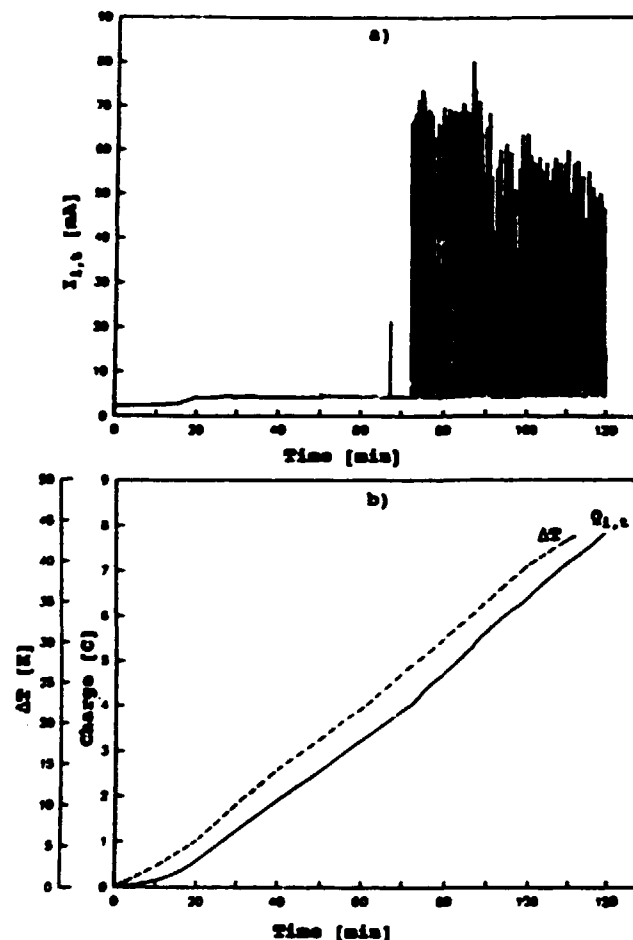


Fig. 6 Method c: example of the trends of electrical and thermal quantities as a function of time.

After a few minutes, the $I_{i,t}$, which is similar to the $I_{o,b}$, reached a base value of a few milliamperes, which remained nearly constant throughout the test. After about one hour, higher peaks, reaching values up to about 80 mA, appeared. The charge records indicated that these high peaks did not contribute significantly to the total charge. This is confirmed by the small variation of the slope of the time trend of the charge $Q_{i,t}$ and of the temperature rise ΔT in correspondence to the high peaks initiation. High ΔT were reached on the non-contaminated unit. The ratio between ΔT and $Q_{i,t}$ was about 6.5 K/C after a test duration of 2 hours.

Tests to analyze the repeatability were made contaminating the bottom unit with a S_{sd} of 0.15 mg/cm^2 and with a test duration of 2 hours.

The average and the standard deviation of the measured values of the maximum ΔT were about 70 K and 34 K respectively.

The spread in the result was lower than for method b), because of the almost imposed voltage unbalance. However it was higher than for method a), due to differences in the humidification process intrinsic in the solid layer tests. The spread in the humidification process has a

relatively low influence on the flashover voltage of external insulation and can therefore be tolerated for insulator testing, but it can remarkably influence the thermal performance of surge arresters.

Tests lasting more than 2 hours did not show much higher ΔT , probably because of the washing out process caused by the steam fog.

Tests with different contamination levels did not show any significant influence of the contamination level on the ΔT , at least in the examined range.

Finally tests were performed contaminating only the top unit (instead of the bottom one). As in method a), the ΔT on the most stressed unit was found a little lower than contaminating the bottom unit only. Furthermore the results were more spread than contaminating the bottom unit only. This fact can be explained considering a possible redistribution of the contaminant along the arrester during the test.

Method d): Solid layer with uniform contamination

The tests were carried out following the same procedure that was adopted for method c), but in this case, the arrester was subjected to uniform contamination. Several tests were performed with S_M values ranging from 0.015 to 0.15 mg/cm². Charge and currents measurements did not indicate preferential activity on the top or bottom unit. The maximum ΔT was quite low (generally lower than 20 K) even for rather high testing times and independently of the contamination level.

Method e): Salt fog test

The tests were carried out according to the procedure reported in (8). The test duration was extended up to 4 hours. Fog salinities, S , varying from 2.5 to 40 kg/m³ were used.

Examples of $Q_{1,b}$, $Q_{1,t}$, $Q_{2,b}$, $Q_{2,t}$ and ΔT trends are shown in Fig. 7, which refers to $S = 14 \text{ kg/m}^3$ and a duration of 3 hours. In the example, the $Q_{1,t}$ at the end of the test reached a value of 12 C, which would correspond to a average value of the current peaks equal to 4.5 mA. Much higher peak values were recorded during the tests (up to 80 mA). High ΔT values were reached on the top unit.

Tests to analyze the repeatability were made with a salinity of $S = 14 \text{ kg/m}^3$ and with a test duration of 2 hours.

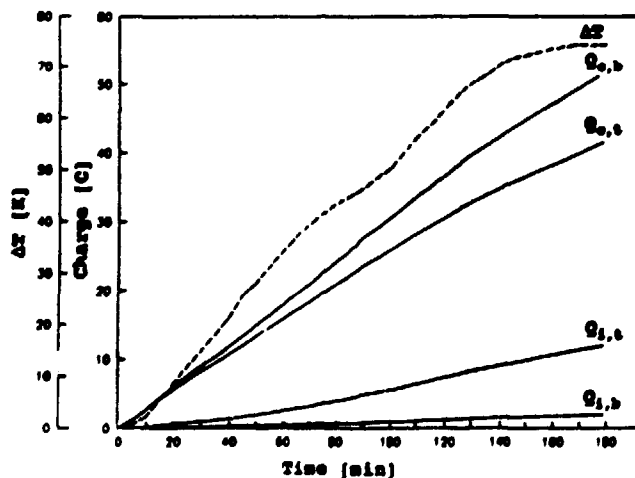


Fig. 7 Method e): example of the trends of electrical and thermal quantities as a function of time.

The total charge ($Q_1 + Q_2$) ranged from 15 to 30 C per hour: the charge (current) of the bottom unit flowed mainly externally, while, on the top unit both external and internal charge were present, with a systematic prevalence of the external one.

The average and the standard deviation of the measured values of the maximum ΔT were of about 105 K and 59 K respectively.

Also for this method the analysis of correlation between the various parameters was made. The maximum ΔT was proportional to $Q_{1,t}$ with a coefficient of 5.5 K/C at the end of a test duration of 3 hours. ΔT showed a very loose correlation with all the other parameters, including $Q_{2,b}$.

Subsequent tests made with different contamination levels (S varying from 2.5 to 40 kg/m³) did not indicate any significant influence of the contamination severity, at least in the examined range.

GENERAL CONSIDERATIONS ABOUT THE TEST METHODS

The pollution tests can be grouped into two main families:

- Those for which the voltage unbalance is forced: namely wet contaminant with the non-uniform contamination (method a)) and solid layer with non-uniform contamination (method c)).
- Those for which the voltage unbalance is not predetermined and results from the pollution dynamic, such as wet contaminant with uniform contamination (method b)), solid layer with uniform contamination (method d)), salt fog (method e)).

Analysis of test repeatability

The cumulative frequency distribution of the maximum ΔT is reported in Fig. 8, where the results obtained with different test methods, in the frame of the tests performed to analyze test repeatability, are reported.

Obviously the first family of tests is characterized by a lower spread in the results. Among them, method a) showed a higher repeatability. For this method few tests are necessary to get close to the relevant maximum severity. For the methods of this family the measurement of the external charge on the contaminated unit gives a good estimate of test severity.

The second family of tests is characterized by a very high spread. For these methods many tests are necessary to get close to the maximum temperature conditions

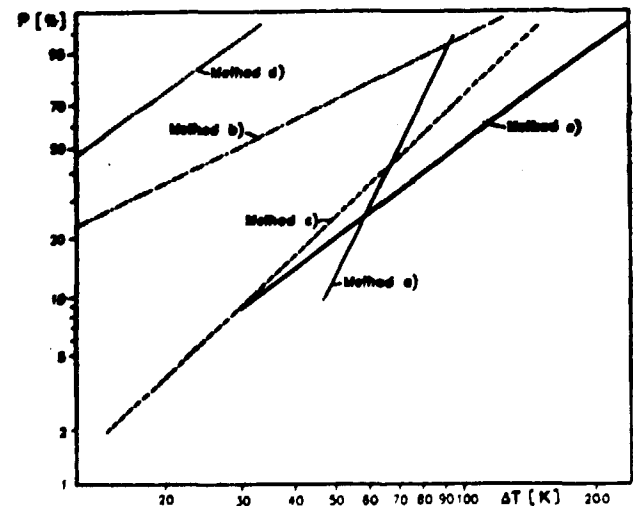


Fig. 8 Cumulative frequency distribution of the maximum ΔT . Data for the different test methods.

typical of the tests. For these methods the external charge is very poorly related to the internal charge on the most stressed unit and thus with its temperature rise.

Analysis of test representativity

The first family of tests may be suitable to represent the most critical field conditions.

In principle, tests of the second family should be more representative of practical conditions, provided the method chosen correctly reproduces actual field conditions.

Analysis of test severity

Some indications about the test severity may be obtained from Fig. 8. However it has to be taken into account that the relative severities of the different test methods are influenced by the somewhat arbitrary choice of test duration or number of contamination cycles.

Generalization of the results obtained

Tests performed on the surge arresters of different ratings and designs considered have given information substantially in line with that obtained on the surge arrester more systematically investigated; in particular similar indications were obtained about the order of merit of the various test procedures and about test repeatability.

SECTION 2: ARRESTER MODELLING UNDER POLLUTION CONDITIONS

TEST OBJECT AND ARRESTER MODELLING

Pollution tests involve quite complicated phenomena and the understanding of the role played by the different parameters in the electrical and thermal performance of surge arresters under pollution is very difficult. The dynamic evolution of the surface conditions during pollution tests is one of the aspects contributing to this difficulty.

A physical model of the surge arrester under pollution conditions was developed in order to simplify the comprehension of the phenomena: different possible surface conditions were simulated statically, by connecting in parallel to the top and/or to the bottom unit of the surge arrester in Fig. 1 external resistors (R_1 and R_2) with different values or by short circuiting parts of the porcelain of the test object by means of metallic foils adjacent to the sheds. The test sample was equipped with the same measuring devices foreseen in Section 1.

The thermal and electrical phenomena were also investigated by means of a mathematical model of the surge arrester under pollution. A short description of the model is reported in the Appendix.

ANALYSIS OF THERMAL PERFORMANCE

During pollution tests, heating was generally observed only in one arrester unit while the other one was practically unaffected by the tests. The temperature rise was not uniform along the axis of the most stressed unit.

Furthermore, the heating process developed with different magnitudes and over different times depending on test method adopted.

The temperature rise profiles along the arrester axis were analysed by means of both models under various conditions. Fig. 9 gives the temperature rise profiles calculated with the mathematical model and measured with the physical model after an energization at constant power losses lasting 80 min and during subsequent cooling. The data refer to the case with a resistor, $R_1 = 6 \text{ M}\Omega$ connected in parallel to the top unit; the relevant power injected in the bottom unit was 370 W.

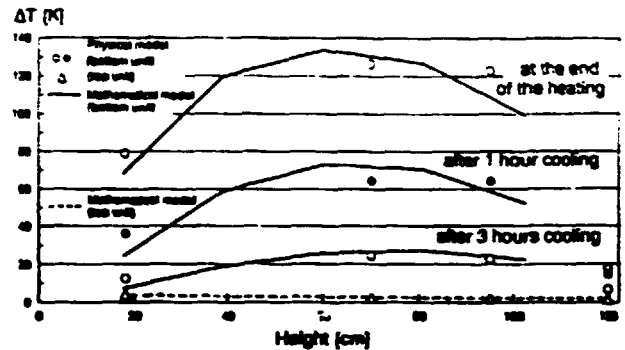


Fig. 9 Temperature rise profiles along the arrester after heating of one unit and subsequent cooling. Results obtained by the analytical model and validated by physical modelling.

High ΔT were observed in the most stressed unit while the temperature on the other one was not affected by the test. Furthermore, the temperature profile on the most stressed unit showed the typical trend found during pollution tests, with the highest temperature in the middle of the unit; this temperature profile can be explained considering that the only significant heat transfer phenomenon is the radial and axial transmission within the arrester unit, while the heat transmission between the two units is negligible.

Heating thermal transients were also analyzed through the models. Examples are given in Fig. 10, showing the ΔT values inside the arrester under three conditions; the data are obtained using the physical and the mathematical models. For high power losses ($P = 2250 \text{ W/arrester unit}$) the heating is very rapid and the transient can be considered to be almost adiabatic while the transient is no longer adiabatic for lower power losses ($P = 210 \text{ W/arrester unit}$) where the heating is much slower. Power losses given continuously ($P = 350 \text{ W/arrester unit}$, with a continuous energization) or discretely ($P = 630 \text{ W/arrester unit}$, with an interruption in the energization of 8 min every 18 min to give the same total energy as in the previous case) give similar results in terms of heating, provided the tin intervals are well below the surge arrester equivalent thermal time constant (about 110 min). The intermittent power input is similar to that which takes place during pollution tests with method a) and b), while the continuous power input simulates pollution tests with method c), d) and e).

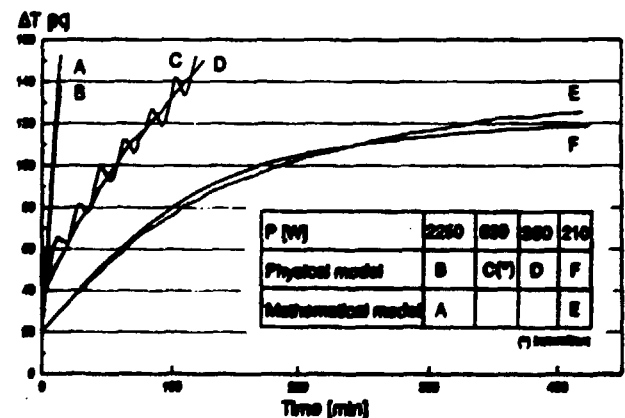


Fig. 10 Examples of thermal transients. Results obtained by analytical model and validated by physical modelling.

ANALYSIS OF ELECTRICAL PERFORMANCE

The pollution test results indicate that the ΔT of the most stressed surge arrester unit is generally not correlated to the maximum current peaks or to the

external charge Q_e . On the other hand, a good correlation exists with its internal charge Q_i . An estimate of Q_i can be obtained measuring the Q_e in the less stressed arrester unit. However when the most stressed unit is not a-priori known, or when the most stressed unit is not the same during the whole test, the measurement of Q_e can not give significant indications about surge arrester heating.

The importance of the internal charge Q_i was analyzed by the models. Calculation and physical modelling confirm, as expected, that a linear relation is obtained when plotting the energy ΔT against the maximum ΔT reached by the arrester in a defined time, as shown in Fig. 11.

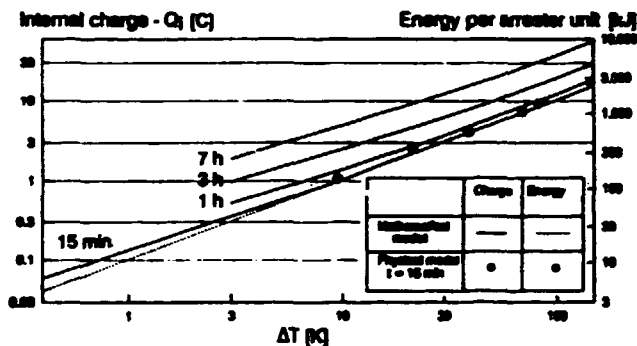


Fig. 11 Dissipated energy and internal charge as a function of ΔT for various testing times. Results obtained by the analytical model and validated by physical modelling.

A similar linear relation is also valid between the charge Q_i and ΔT at least for charge per unit time values higher than about 1 C/hour. This fact can be explained considering that, above a certain current, the voltage applied to the resistor blocks is nearly constant and close to the value corresponding to the knee of the volt-ampere characteristics of the blocks, as shown in Fig. 12. Then, the Q_i can be adopted as a good estimate of the energy responsible for arrester heating. The same cannot be applied to Q_e . Finally, the data in Fig. 11 indicate that the charge (energy) necessary to reach a defined temperature increases when the testing time is increased because the process deviates from the adiabatic behaviour. Correspondingly the ratio $\Delta T/Q_i$ decreases. The results obtained during the pollution tests are well in agreement with those obtained by modelling.

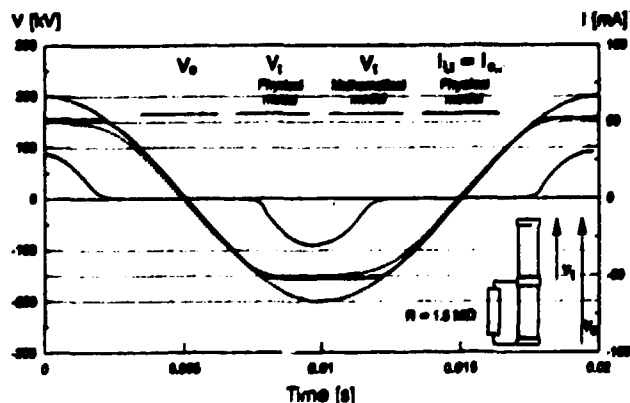


Fig. 12 Voltage and current waveshape in the most stressed unit. Results obtained by analytical model and validated by physical modelling.

INFLUENCE OF SURFACE CONDITIONS ON ARRESTER PERFORMANCE

The pollution tests performed show that the heating of the arrester is related to the unbalance of the surface resistance on the arrester units and the quantity of water to be vaporized to dry the contamination layer, while it is not significantly related to the pollution level.

Systematic applications of the models were performed to help clarify these trends.

In the physical modelling, the top and the bottom unit were alternately short-circuited by metallic foils adhering to the porcelain profile. Fig. 13 reports the internal current I_i and charge Q_i on both arrester units, as a function of the length of porcelain short-circuited on the bottom unit. A noticeable increase in charge and current was observed only with the total short-circuit of the unit (made, limitedly to this case by 1.5 MΩ resistor, to prevent failure of the test object). Therefore, the only significant current exchange between the inside and the surface of the surge arrester occurred at intermediate flanges. The current drained by stray capacitance was negligible, at least in the examined case with a limited capacitance between resistor blocks and porcelain surface (about 50 pF/m). Higher influences could be expected for arrester designs with much higher radial capacitance. However this influence would be limited by the relatively low frequencies present in the current spectrum.

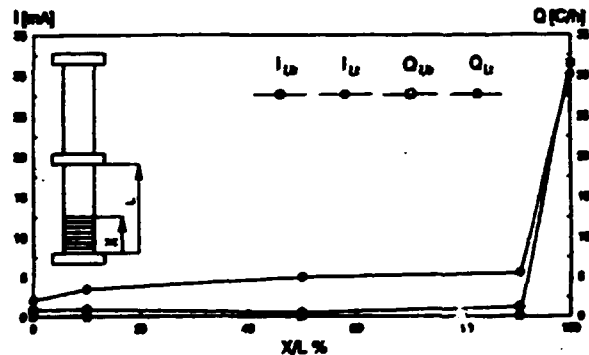


Fig. 13 Influence of local surface conditions on arrester performance. Results obtained by physical modelling.

The results show that the local resistivity along the surge arrester unit surface is of minor importance, while the significant parameter is the overall surface resistance of the unit. These results also explain the low thermal stress to which single unit surge arresters are exposed to under contamination conditions.

The influence of the total surface resistance of a surge arrester unit on the internal power losses was also analyzed: Fig. 14 reports the result of physical modelling and calculations. The internal power losses in the bottom unit of the surge arrester are given in the Figure as a function of the ratio of the value of the resistances R_1 and R_2 connected in parallel respectively to the bottom and to the top unit. Various curves were obtained for different R_2 values. In the cases illustrated in Fig. 14, with $R_2 > R_1$, the power losses on the top unit were negligible and those in the bottom unit increased when the ratio R_1/R_2 was increased. For a fixed ratio R_1/R_2 , the power losses increased when R_2 was decreased (aiming to simulate an increase in the contamination level).

The models confirm that the most severe contamination tests are those characterized by very different conductivity conditions between units (e.g. when one unit is contaminated and wetted and the other one is totally or partially dried).

The models also indicate a remarkable influence of the layer resistance on heating, which is not confirmed by

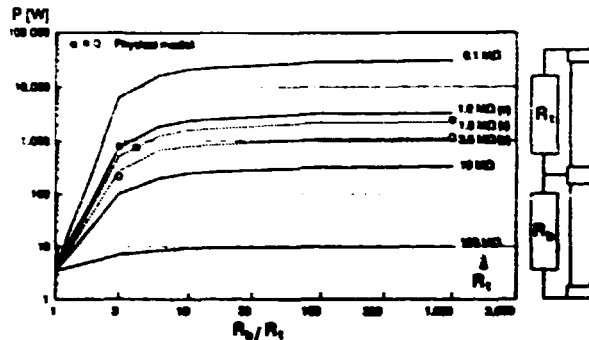


Fig. 14 Influence of the surface condition of the units on arrester performance. Results obtained by analytical modelling (lines) and validated by physical modelling (symbols).

the tests. Actually, static modelling do not simulate the dynamic evolution of the resistivity which occurs in pollution tests (see Fig. 2a and 2b). The worst condition for a multiple-unit arrester is when one unit is much less conductive than the other one (because of a natural dry band as in the salt fog method or because of a prefixed dry band as in method a) and c)). In this case the charge which flows internally in the unit with the dry bands has to flow externally on the other unit and will flow up to the drying of the layer itself. The charge necessary to dry the layer is a function of the layer geometry and wetting condition and to a lesser degree of the layer conductivity, provided that the pollution condition is well below that leading to external flashover.

CONCLUSIONS

The comparison of the results obtained with the different laboratory test methods reported in Section 1 indicates that:

- The thermal performance of surge arresters under contaminated conditions mainly depends on the contamination unbalance among the arrester units and on the wetting condition while it is practically unaffected by contamination level.
- The pollution tests which force a contamination (voltage) unbalance are the most repeatable. In particular the ANSI method showed fairly good repeatability.
- The pollution methods which do not force the voltage unbalance (those with uniform contamination and salt fog method) may be more representative of actual conditions, but are less repeatable. Their standardisation implies to perform a large number of tests on each object.
- The arrester heating is related to the charge which flows in the arrester blocks. The charge flowing on the housing (external charge) has a very loose relation with arrester thermal stress, unless when it coincides with the internal charge; this occurs in the methods with a fixed contamination unbalance.

Physical and mathematical modelling reported in Section 2 confirmed the above conclusions and indicated that:

- The only significant heat transfer phenomenon are the radial and axial transmission within the surge arrester units, while the transmission between the units is negligible.
- The only significant current exchange between the inside and the housing of the surge arrester occurs at intermediate flanges. The local resistivity along the surge arrester housing is then of minor importance, and the significant parameter is the overall surface resistance of the unit.
- The internal charge is directly related to the energy dissipated inside the surge arrester and thus to the

temperature. The charge is a function of the layer geometry and of the wetting conditions and to a lesser degree of the pre-fired layer conductivity.

APPENDIX

Description of the mathematical model of the arrester

Arrester modelling can be very useful to obtain indications about electrical and thermal performance of surge arresters [10], [11].

A mathematical model of the arrester was implemented to simulate the arrester electrical and thermal performance under polluted conditions.

The aim of the electrical model was to evaluate the power losses inside the arrester under a given surface contamination condition, by calculation of the voltage and current distribution along the arrester.

The purpose of the thermal model was to evaluate the heating time trend of the various arrester parts: the input was the local electric power losses, as computed by the electric model.

The two models were closely interfaced using an appropriate software, to allow step by step calculations, taking into account the variation of the volt-ampere characteristics of the resistors with temperature. The transient solutions of both models were obtained through an MTF package.

Electrical model

The surge arrester was simulated from the electric point of view by means of an electric network with lumped parameters. Figure A1 details a non-edge portion of the equivalent circuit. In particular:

- The metal oxide resistors were described through a non-linear resistance, R_1 , and capacitance, C_1 . The values of the parameters were derived experimentally.
- Stray capacitances between blocks and porcelain housing, C_{1p} , between porcelain and the ring, C_{2p} , and between porcelain and earth, C_{3p} , were evaluated on the basis of the geometry of the system through electric field calculation programs.
- Surface resistances, R_2 , of the insulator housing were assigned on the basis of the phenomenon considered; in a given instant a contaminated zone of the arrester can be wetted, dried to form a dry zone and eventually short-circuited by a discharge. Resistance values which differed by several orders of magnitude were assigned to the various zones of the porcelain housing to take into account specific surface conditions. Terminal parts were represented by appropriate circuit components.

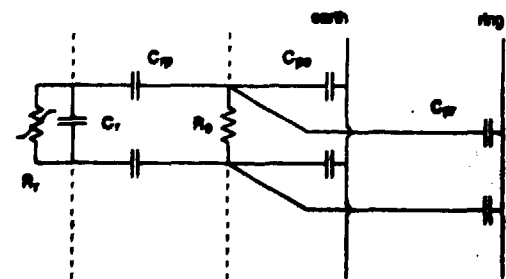


Fig. A1 Electrical model: non-edge portion of the equivalent circuit of the surge arrester.

Thermal model

The simulation of the thermal behaviour was made through an equivalent electrical network with lumped parameters.

Figure A2 shows a non-edge portion of the equivalent circuit. In particular:

- Heat generation was represented by current generators, P_1 and P_2 , with the numerical current value equal to that of the power losses respectively inside and on

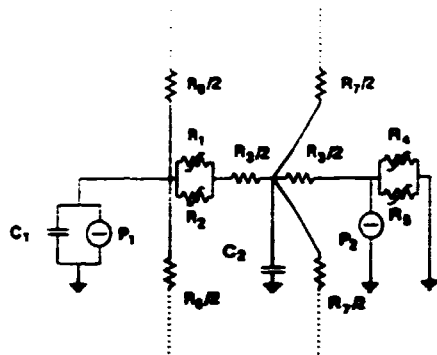


Fig. A2 Thermal model: non-edge portion of the equivalent circuit of the surge arrester.

- the surface of the arrester.
- Thermal capacitances of the resistors and of the porcelain were represented respectively by the capacitors C_1 and C_2 .
- Radial heat transfer between the blocks and porcelain was described through the non-linear resistors R_1 and R_2 , handling respectively radiation and convection.
- Radial heat transfer inside the porcelain was simulated through the resistor R_3 , handling conduction.
- Radial heat transfer between the porcelain and the ambient was simulated through the non-linear resistors R_4 and R_5 , handling respectively radiation and convection. They were evaluated on the basis of a physical relation.
- Axial heat transfer was described by the resistor R_6 and R_7 , expressing respectively conduction inside the resistors and porcelain.

The various parameters were evaluated through a physical relation based on the geometry of the configuration and material characteristics.

Terminal parts were represented by appropriate circuit components (taking into account the thermal behaviour of the flanges).

ACKNOWLEDGEMENTS

Many thanks are due to Prof. Gianpaolo Carrara for useful discussions and advice.

REFERENCES

- [1] A. Bargigia, L. Giannuzzi, A. Inesi, A. Porriano, A. Figini, L. Thione "Study of the performance of Metal Oxide Arresters for High Voltage Systems" CIGRE 1986, Report 33-14
- [2] M. de Nigris "The impact of pollution on high voltage surge arresters" CPRI Workshop on pollution performance of insulators, Bangalore, India, 25th sept. 1987
- [3] A. Bargigia, G. Nassa, G. Le Roy, A. Rousseau, L. Sparrow "Behaviour of Metal Oxide Surge Arrester under different environmental conditions" CIGRE 1988, Report 33-07
- [4] J. Lundquist, L. Stenstrom, S. Vitet "Thermal stress on ZnO surge arresters in polluted conditions: Part I: Laboratory test methods" IEEE paper 91 WM 013-3 PWRD
- [5] J. Lundquist, A. Schei, L. Stenstrom, S. Vitet "Thermal stress on ZnO surge arresters in polluted conditions: Part II: Field test results" IEEE paper 91 WM 014-1 PWRD
- [6] ANSI/IEEE C62.11-1987 "IEEE Standard for Metal-Oxide Surge Arresters for AC Power Circuits"
- [7] CIGRE 33 (TF04-06) "Proposal for an artificial pollution test on Metal Oxide Surge Arresters" 33(TF04-06) 1990 doc. 24 IWD (Private commun.)
- [8] IEC Publication 507 (1990) "Artificial pollution tests on high voltage insulators to be used on a.c. systems"

- [9] S. Yakov (on behalf of CIGRE WG 15.01.02) "Statistical Analysis of dielectric test results" CIGRE Technical Brochure 1991
- [10] M.V. Lat "Analytical method for performance prediction of metal oxide arresters" IEEE Trans. on Power Apparatus and Systems, Vol. PAS-104 N. 7, July 1985
- [11] G. St-Jean, A. Petit "Metal oxide surge arrester operating limits defined by a temperature margin concept" IEEE Trans. on Power Delivery, Vol. 5 N. 2, April 1990



Annale Bargigia, born in Milan (Italy) in 1950, received the Doctor's degree in Electrical Engineering from the Milan Polytechnic in 1975. After a period of research activity on Electrical Machines and Measuring Techniques with the same Institute, he joined the Electrical Research Centre of ENEL where he now heads the section "Switchgears, Controlgears and Surge Arresters". Within the framework of the 1000 kV ENEL Project he is a member of the Research and Installation Group "Substations". He is an active member of various Working Groups of CIGRE SC 13 and 33 and IEC TC 17 and 37. He is the author of several international reports.



Michele de Nigris, (M '90) born in Brussels (Belgium) in 1959, received the Doctor's degree from the University of Genoa (Italy) in 1983. He joined CESI in 1984. His main areas of interest are overvoltage protection with arresters and studies about the evaluation of the residual life of power plant electrical components. He is secretary of TC 37 "Surge arresters" and of SC37A "Low voltage SPD" of the Italian Electrotechnical Committee (CEI). He is a Member of IEEE and AIEE. He is the author or co-author of several national and international reports.



Alberto Fianini (M' 85 - SM' 86), born in Castell'Gardone, Italy, in 1946, received the Doctor's degree in Electrical Engineering from the Milan Polytechnic in 1971. He joined CESI in 1972 where he started his activity in the field of high voltage research, dealing with internal and external insulation, apparatus, measuring and testing techniques. He now heads the section of High Voltage and High Power Divisions of CESI dealing with Research and Development. He is a Member of AIEE and CIGRE and Senior Member of IEEE. He is the author or co-author of several national and international reports.



Alberto Sirani, born in Lecco (Italy), in 1962, received the Doctor's degree in Electrical Engineering from the Milan Polytechnic in 1988. In 1990 he joined CESI where he conducts research in the high voltage field. At present his main field of interest is surge arresters, with special reference to their behaviour under contamination conditions.

MICROCOPY RESOLUTION TEST CHART
 NATIONAL BUREAU OF STANDARDS-
 STANDARD REFERENCE MATERIAL 1919A
 (ANSI AND ISO TEST CHART NO. 2)

